

# NAC-TDDFT: Time-dependent density functional theory for nonadiabatic couplings

Zikuan Wang, Chenyu Wu and Wenjian Liu\*

*Qingdao Institute for Theoretical and Computational Sciences, Institute of Frontier and Interdisciplinary Science, Shandong University, Qingdao, Shandong 266237, China*

E-mail: liuwj@sdu.edu.cn

## Conspectus

First-order nonadiabatic coupling matrix elements (fo-NACMEs) are the basic quantities in theoretical descriptions of electronically nonadiabatic processes that are ubiquitous in molecular physics and chemistry. Given the large size of systems of chemical interests, time-dependent density functional theory (TDDFT) is usually the first choice. However, the lack of wave functions in TDDFT renders the formulation of NAC-TDDFT for fo-NACMEs conceptually difficult. The present account aims to analyze the available variants of NAC-TDDFT in a critical but concise manner and meanwhile point out the proper ways for implementation. It can be concluded, from both theoretical and numerical points of view, that the equation of motion-based variant of NAC-TDDFT is the right choice. Possible future developments of this variant are also highlighted.

## 1 Introduction

Electronically nonadiabatic processes involving more than one Born-Oppenheimer (BO) potential energy surfaces (PES) are ubiquitous in chemistry, biology and materials science.

There exist two mechanisms for these to happen, purely electronic and finite nuclear mass effects. The former refers to spin-orbit couplings (SOC) responsible for transitions between electronic states of different spins, whereas the latter to derivative couplings causing transitions between electronic states of the same spin. To see the latter, we start with the (clamped nuclei) electronic Schrödinger equation

$$H_e|\Psi_I(\{\mathbf{r}_i\}; \{\mathbf{R}_A\})\rangle = E_I(\{\mathbf{R}_A\})|\Psi_I(\{\mathbf{r}_i\}; \{\mathbf{R}_A\})\rangle, \quad (1)$$

$$H_e = T_e + V_{nn}(\{\mathbf{R}_A\}) + V_{ne}(\{\mathbf{r}_i\}; \{\mathbf{R}_A\}) + V_{ee}(\{\mathbf{r}_i\}), \quad (2)$$

where the semi-colons emphasize that the nuclear coordinates  $\{\mathbf{R}_A\}$  are parameters instead of variables like the electronic coordinates  $\{\mathbf{r}_i\}$ . The eigenvalues  $E_I(\{\mathbf{R}_A\})$  form PESs on which the nuclei move. Since  $\{|\Psi_I(\{\mathbf{r}_i\})\rangle\}$  form a complete basis set (CBS), the total wave function can be expanded as

$$\Phi(\{\mathbf{r}_i\}, \{\mathbf{R}_A\}) = \sum_J \Theta_J(\{\mathbf{R}_A\})\Psi_J(\{\mathbf{r}_i\}; \{\mathbf{R}_A\}), \quad (3)$$

which can be inserted into the full Schrödinger equation

$$(T_n + H_e)\Phi(\{\mathbf{r}_i\}, \{\mathbf{R}_A\}) = E_{\text{tot}}\Phi(\{\mathbf{r}_i\}, \{\mathbf{R}_A\}) \quad (4)$$

to obtain the nuclear Schrödinger equation

$$(T_n + E_I(\{\mathbf{R}_A\}))\Theta_I(\{\mathbf{R}_A\}) + \sum_J H_{IJ}^{\text{BO}}\Theta_J(\{\mathbf{R}_A\}) = E_{\text{tot}}\Theta_I(\{\mathbf{R}_A\}), \quad (5)$$

where

$$H_{IJ}^{\text{BO}} = - \sum_{\xi} \frac{1}{M_{\xi}} (g_{IJ}^{\xi} \partial_{\xi} + h_{IJ}^{\xi}), \quad \partial_{\xi} = \frac{d}{d\xi} \quad (6)$$

$$g_{IJ}^{\xi} = \langle \Psi_I | \partial_{\xi} | \Psi_J \rangle, \quad (7)$$

$$h_{IJ}^{\xi} = \frac{1}{2} \langle \Psi_I | \partial_{\xi}^2 | \Psi_J \rangle. \quad (8)$$

Here,  $\xi$  runs over all nuclear degrees of freedom and  $M_{\xi}$  is the corresponding atomic mass. Clearly, the matrix operator  $H_{IJ}^{\text{BO}}$  vanishes in the limit of infinite nuclear masses. Conversely, for the true atomic masses, the operator will induce transitions between electronic states of the same spin, especially when the states are energetically adjacent (cf. Eq. (10) below). Since the second-order nonadiabatic coupling matrix elements (NACME) (8) can be “transformed away” (without approximation for the considered manifold of PESs) by replacing the canonical with the kinematic nuclear momentum,<sup>1</sup> only the first-order (fo) NACMEs (7) are relevant. In view of the relation

$$\langle \Psi_I | [\partial_{\xi}, H_e] | \Psi_J \rangle = \omega_{JI} g_{IJ}^{\xi}, \quad \omega_{JI} = E_J - E_I, \quad \forall I \neq J, \quad (9)$$

the fo-NACMEs can be calculated as

$$g_{IJ}^{\xi} = \frac{\langle \Psi_I | V_{\text{ne}}^{\xi} | \Psi_J \rangle}{\omega_{JI}} = -g_{JI}^{\xi}, \quad V_{\text{ne}}^{\xi} = [\partial_{\xi}, V_{\text{ne}}] = (\partial_{\xi} V_{\text{ne}}) \quad (10)$$

$$= \frac{1}{\omega_{JI}} \sum_{pq} \langle \psi_p | V_{\text{ne}}^{\xi} | \psi_q \rangle \gamma_{pq}^{IJ}, \quad \gamma_{pq}^{IJ} = \langle \Psi_I | a_p^{\dagger} a_q | \Psi_J \rangle. \quad (11)$$

Use of the above Hellmann-Feynman-like expression was first made by Chernyak and Mukamel<sup>2</sup> for the fo-NACMEs between the ground and excited states (*ge*) in the context of time-dependent density functional theory (TDDFT), which does provide reduced transition density matrices (rTDM)  $\gamma^{IJ}$  between a pair of states. However, even ignoring the fact that the expression (11) is rooted in (exact) wave function theory (WFT) and hence incompatible

with TDDFT, it is hardly useful in practice, for it requires a CBS. For atom-centered basis sets, the convergence is extremely slow, which can easily be understood by noticing that, as a real-space function,  $V_{\text{ne}}^{\xi}$  has a dipole symmetry and behaves as  $R^{-2}$  in the vicinity of the nucleus. As such, not only steep  $p$  functions but also functions of angular momentum  $l + 1$  have to be added to standard basis functions of angular momentum  $l$ .<sup>3</sup> A more useful and simple approach is the finite difference approximation via fast evaluation of the overlap integrals between electronic wave functions at displaced geometries.<sup>4,5</sup> However, in total  $6N_{\text{atom}}$  evaluations of the overlap integrals are needed to get the fo-NACMEs and care has to be taken of the dependence on geometric displacements as well as the phase alignment of the wave functions. Therefore, analytic NAC-TDDFT should be formulated (see Sec. 2) and recast into practically useful forms (see Sec. 3). Some numerical results will be provided in Sec. 4 before concluding the Account in Sec. 5.

The following convention is to be used:  $\{i, j, k, l\}$ ,  $\{a, b, c, d\}$  and  $\{p, q, r, s\}$  denote occupied, virtual and arbitrary molecular orbitals (MO), whereas Greek letters refer to atomic orbitals (AO).

## 2 NAC-TDDFT

Under the adiabatic approximation, TDDFT amounts to solving the following eigenvalue problem<sup>6</sup>

$$\mathbf{E}\mathbf{t}_I = \omega_I\mathbf{S}\mathbf{t}_I, \quad \mathbf{t}_I^\dagger\mathbf{S}\mathbf{t}_J = \delta_{IJ}, \quad (12)$$

where

$$\mathbf{E} = \begin{pmatrix} \mathbf{A} & \mathbf{B} \\ \mathbf{B} & \mathbf{A} \end{pmatrix}, \quad \mathbf{S} = \begin{pmatrix} \mathbf{I} & \mathbf{0} \\ \mathbf{0} & -\mathbf{I} \end{pmatrix}, \quad \mathbf{t}_I = \begin{pmatrix} \mathbf{X}_I \\ \mathbf{Y}_I \end{pmatrix}, \quad (13)$$

$$A_{ia\sigma,jb\tau} = \delta_{\sigma\tau}(\delta_{ij}F_{ab\sigma} - \delta_{ab}F_{ji\sigma}) + K_{ia\sigmajb\tau}, \quad (14)$$

$$B_{ia\sigma,jb\tau} = K_{ia\sigmabj\tau}, \quad (15)$$

$$K_{pq\sigma,rs\tau} = (pq\sigma|sr\tau) - c_x\delta_{\sigma\tau}(pr\sigma|sq\sigma) + c_{xc}f_{pq\sigma sr\tau}^{xc}[\rho], \quad (16)$$

$$F_{\mu\nu\sigma} = h_{\mu\nu} + \sum_{i\tau} [(\mu\sigma\nu\sigma|i\tau i\tau) - c_x\delta_{\sigma\tau}(\mu\sigma i\tau|i\tau\nu\sigma)] + c_{xc}v_{\mu\nu\sigma}^{xc}[\rho], \quad h_{\mu\nu} = T_{\mu\nu} + (V_{ne})_{\mu\nu}. \quad (17)$$

Here,  $\sigma$  and  $\tau$  are spin indices. One major issue here is that the eigenvectors of Eq. (12) do not correspond to excited-state wave functions, but are related to the TDM describing linear response of the ground state density to an external field (cf. equation (103) in Ref. 7). The lack of wave functions renders the formulation of TDDFT for fo-NACMEs at least formally difficult. In the next subsections, the auxiliary/pseudo wave function (AWF), equation of motion (EOM), and time-dependent response/perturbation theory (TDPT) based formulations are analyzed sequentially.

## 2.1 AWF-based formulation

To draw analogy with WFT, we start with the Tamm-Dancoff approximation (TDA) to Eq. (12),

$$\mathbf{A}\mathbf{X}_I = \omega_I\mathbf{X}_I. \quad (18)$$

If Hartree-Fock (HF) is used as the functional, the  $\mathbf{A}$  matrix (14) is just the Hamiltonian matrix in the manifold of singly excited configurations  $\{|\Psi_i^a\rangle = a_a^\dagger a_i |\Psi_{\text{HF}}\rangle\}$ . Therefore, in this case, the eigenvector  $\mathbf{X}_I$  represents simply the coefficients of the CIS (configuration interaction singles) wave function  $\Psi_I^{\text{CIS}}$ ,

$$|\Psi_I^{\text{CIS}}\rangle = \sum_{ia} |\Psi_i^a\rangle (\mathbf{X}_I)_{ia}. \quad (19)$$

Extending the above to an arbitrary functional leads to

$$|\Psi_I^{\text{TDA}}\rangle = \sum_{ia} (\mathbf{X}_I)_{ia} a_a^\dagger |\Psi_{\text{KS}}\rangle, \quad (20)$$

which can be termed ‘‘auxiliary wave function’’ (AWF). In this way, the *ge* and *ee* (excited state-excited state) fo-NACMEs can readily be obtained as

$$g_{0I}^\xi = \sum_{ia} \langle \psi_i | \partial_\xi | \psi_a \rangle (\mathbf{X}_I)_{ia}, \quad (21)$$

$$g_{IJ}^\xi = \sum_{iab} (\mathbf{X}_I)_{ia} (\mathbf{X}_J)_{ib} \langle \psi_a | \partial_\xi | \psi_b \rangle - \sum_{ija} (\mathbf{X}_I)_{ia} (\mathbf{X}_J)_{ja} \langle \psi_j | \partial_\xi | \psi_i \rangle. \quad (22)$$

However, these are not yet the final working equations, as they involve nuclear derivatives of the MOs, which must be either calculated directly from coupled-perturbed KS (CPKS) equations or eliminated by the Z-vector approach (see Sec. 3).

The situation becomes very different for the full TDDFT, which has no direct analogy with any WFT. One common practice is to construct a CIS-like wave function that reproduces some property (e.g., electric polarizability) in a sum-of-states form, and then feed it to Eq. (7). Different choices of properties then lead to different expressions, e.g.,

$$g_{0I}^\xi = \sum_{ia} (\mathbf{X}_I + \mathbf{Y}_I)_{ia} \langle \psi_i | \partial_\xi | \psi_a \rangle, \quad (23)$$

and

$$g_{0I}^\xi = \sum_{ia} (\mathbf{X}_I - \mathbf{Y}_I)_{ia} \langle \psi_i | \partial_\xi | \psi_a \rangle, \quad (24)$$

were proposed by Tavernelli<sup>8</sup> and Hu,<sup>9,10</sup> respectively, for the *ge* fo-NACMEs. Even more choices are possible for the *ee* fo-NACMEs.<sup>8,11,12</sup> Due to the lack of theoretical rigor, there is no *a priori* argument to favor one over another. In particular, there is no *a priori* guarantee that any of them is exact if both the functional and kernel were exact. It is shown in the next subsections that NAC-TDDFT can indeed be formulated more properly.<sup>13–17</sup>

## 2.2 EOM-based formulation

In the EOM formalism,<sup>18</sup> one defines an excitation operator  $O_I^\dagger$  that promotes the ground state to an excited state

$$|I\rangle = O_I^\dagger|0\rangle, \quad (25)$$

and is subject to the killer condition

$$\langle 0|O_I^\dagger = 0. \quad (26)$$

After determining  $O_I^\dagger$  by the EOM

$$\frac{1}{2}\langle 0|[\delta O_I, [H_e, O_I^\dagger]] + [[\delta O_I, H_e], O_I^\dagger]|0\rangle = \omega_I \langle 0|[\delta O_I, O_I^\dagger]|0\rangle, \quad \omega_I = E_I - E_0, \quad (27)$$

the *ge* and *ee* matrix elements of an arbitrary operator  $O$  can be calculated as

$$\langle 0|O|I\rangle = \langle 0|OO_I^\dagger|0\rangle \quad (28)$$

$$= \langle 0|[O, O_I^\dagger]|0\rangle, \quad (29)$$

$$\langle I|O|J\rangle = \langle 0|O_I O O_J^\dagger|0\rangle \quad (30)$$

$$= \frac{1}{2}\langle 0|[O_I, [O, O_J^\dagger]] - [[O, O_I], O_J^\dagger]|0\rangle, \quad I \neq J. \quad (31)$$

Note that use of the killer condition (26) has been made when going from Eq. (28)/(30) to (29)/(31), to be consistent with the structure of Eq. (27).

Consider, e.g., the random phase approximation (RPA) with

$$O_I^\dagger = \sum_{ia} (\mathbf{X}_I)_{ia} a_a^\dagger a_i - (\mathbf{Y}_I)_{ia} a_i^\dagger a_a. \quad (32)$$

It can readily be checked that Eq. (27) with (32) is just Eq. (12) with  $c_x = 1$  and  $c_{xc} = 0$ , which can simply be translated to TDDFT with a functional other than HF. Note, however,

the  $O_I^\dagger$  operator (32) does not satisfy the killer condition due to the presence of  $a_i^\dagger a_a$ . As such, in principle Eqs. (28) and (30) should be used for the RPA/TDDFT *ge* and *ee* matrix elements, respectively. The resulting expressions are then the same as those by the previous CIS/TDA-based approach. The very trick for nonvanishing deexcitation amplitudes  $\mathbf{Y}_I$  is still to use Eqs. (29) and (31). Straightforward derivations then yield

$$\langle I|O|J\rangle = \langle I|O|J\rangle_0 + \langle I|O|J\rangle_1, \quad (33)$$

$$\langle I|O|J\rangle_0 = \sum_{pq} \tilde{\gamma}_{pq}^{IJ} \langle \psi_p | O | \psi_q \rangle, \quad (34)$$

$$\langle I|O|J\rangle_1 = \frac{1}{2} \langle 0 | [O_I, [O, O_J^\dagger]_1] - [[O, O_I]_1, O_J^\dagger] | 0 \rangle, \quad (35)$$

$$[O, O_J^\dagger]_1 = \sum_{ia} [O, (\mathbf{X}_I)_{ia}] a_a^\dagger a_i - [O, (\mathbf{Y}_I)_{ia}] a_i^\dagger a_a. \quad (36)$$

where  $\langle I|O|J\rangle_1$  appears only if  $O$  contains nuclear derivatives, and the *ge* and *ee* TDMs are defined in Eqs. (37) and (38), respectively,

$$\tilde{\gamma}_{ia}^{0I} = (\mathbf{X}_I)_{ia}, \quad \tilde{\gamma}_{ai}^{0I} = (\mathbf{Y}_I)_{ia}, \quad \tilde{\gamma}_{ij}^{0I} = \tilde{\gamma}_{ab}^{0I} = 0, \quad (37)$$

$$\tilde{\gamma}_{ij}^{IJ} = - \sum_a [(\mathbf{X}_J)_{ia} (\mathbf{X}_I)_{ja} + (\mathbf{Y}_I)_{ia} (\mathbf{Y}_J)_{ja}], \quad (38a)$$

$$\tilde{\gamma}_{ab}^{IJ} = \sum_i [(\mathbf{X}_I)_{ia} (\mathbf{X}_J)_{ib} + (\mathbf{Y}_J)_{ia} (\mathbf{Y}_I)_{ib}], \quad (38b)$$

$$\tilde{\gamma}_{ia}^{IJ} = \tilde{\gamma}_{ai}^{IJ} = 0. \quad (38c)$$

Some remarks are in order.

- (1) It is the use of the nested commutators of the form  $[O_I, [O, O_J^\dagger]]$  that allows the deexcitation amplitudes  $\mathbf{Y}_I$  to contribute to the matrix elements of  $O$ . Such commutators are only present in EOM but not in the Schrödinger equation itself, which explains the difficulty of formulating a unique AWF for TDDFT, except for the TDA variant.



- (2) The  $ge$  transition matrix element  $\langle 0|O|I\rangle_0$  defined by Eqs. (34) and (37) can be simplified to

$$\langle 0|O|I\rangle_0 = \sum_{ia} (\mathbf{X}_I + \mathbf{Y}_I)_{ia} \langle \psi_i | O | \psi_a \rangle \quad (39)$$

if  $O$  is real Hermitian or to

$$\langle 0|O|I\rangle_0 = \sum_{ia} (\mathbf{X}_I - \mathbf{Y}_I)_{ia} \langle \psi_i | O | \psi_a \rangle \quad (40)$$

if  $O$  is real anti-Hermitian. The important corollary is that, in the AWF-based approach, one should construct the AWF with  $\mathbf{X}_I + \mathbf{Y}_I$  in the case of  $O = V_{\text{ne}}^\xi$  or  $\mathbf{r}$  but with  $\mathbf{X}_I - \mathbf{Y}_I$  in the case of  $O = \partial_\xi$ . This is related to the well-known fact that  $\mathbf{A} + \mathbf{B}$  serves as the orbital Hessian for responses to a real (“electric”) perturbation, whereas  $\mathbf{A} - \mathbf{B}$  for responses to a purely imaginary (“magnetic”) perturbation (which is related to real anti-Hermiticity scaled by the imaginary factor  $i$ ). As such, TDDFT does not admit a unique AWF,<sup>19,20</sup> as the form of the AWF depends on the type of perturbation studied. The AWF constructed to reproduce the dipole polarizability (i.e.,  $\mathbf{X}_I + \mathbf{Y}_I$ ) gives rise to incorrect  $ge$  fo-NACMEs in view of Eq. (40) with  $O = \partial_\xi$ , whereas the same AWF used for  $\langle \Psi_I | V_{\text{ne}}^\xi | \Psi_J \rangle$  in Eq. (11) will yield the correct fo-NACMEs, but only in the CBS limit.

- (3) None of the AWF-based methods can reproduce the  $ee$  fo-NACMEs obtained by EOM, unless further approximations are made.<sup>12</sup> For example, starting with an AWF  $\mathbf{X}_I \pm \mathbf{Y}_I$ , one obtains

$$\langle I|O|J\rangle_0 = \sum_{iab} (\mathbf{X}_I \pm \mathbf{Y}_I)_{ia} (\mathbf{X}_J \pm \mathbf{Y}_J)_{ib} \langle \psi_a | O | \psi_b \rangle - \sum_{ija} (\mathbf{X}_I \pm \mathbf{Y}_I)_{ia} (\mathbf{X}_J \pm \mathbf{Y}_J)_{ja} \langle \psi_j | O | \psi_i \rangle, \quad (41)$$

which involves cross terms like  $(\mathbf{X}_I)_{ia} (\mathbf{Y}_J)_{ib}$  not present in the EOM expression (see Eqs. (34) and (38)).

(4) The second term in Eq. (33) with  $O = \partial_\xi$  has been derived before<sup>13</sup> and is hence not repeated here. The final expressions for the *ge* and *ee* fo-NACMEs read

$$\langle 0|\partial_\xi|I\rangle = \sum_{ia}(\mathbf{X}_I - \mathbf{Y}_I)_{ia}\langle\psi_i|\partial_\xi|\psi_a\rangle, \quad (42)$$

$$\langle I|\partial_\xi|J\rangle = \sum_{pq}\tilde{\gamma}_{pq}^{IJ}\langle\psi_p|\partial_\xi|\psi_q\rangle + \omega_{JI}^{-1}\mathbf{t}_I^\dagger(\partial_\xi\mathbf{E})\mathbf{t}_J. \quad (43)$$

Clearly, the AWF-based expression (24)<sup>9,10</sup> happens to be correct but the expression (23)<sup>8</sup> should be rejected.

Albeit elegant, the above EOM-based formulation of fo-NACMEs is still not satisfactory, for the killer condition (26) does not hold strictly. By contrast, the TDPT-based formulation<sup>13</sup> of NAC-TDDFT is more rigorous, as detailed in the next subsection.

## 2.3 TDPT-based formulation

Apart from the previous time-independent AWF and EOM formulations, NAC-TDDFT can also be formulated<sup>13,14</sup> through TDPT, which describes the changes of the ground state to a time-dependent perturbation

$$V(t) = \sum_k e^{-i\omega_k t} \sum_\beta V^\beta(\omega_k)\epsilon_\beta(\omega_k), \quad (44)$$

where  $V^\beta(\omega_k)$  is the perturbation operator with strength  $\epsilon_\beta(\omega_k)$ . Under this perturbation, the ground state is also dependent on time, i.e.,  $|0\rangle = |0(t)\rangle$ . Since we are only interested in the evolution of a ground state property, e.g.,  $\langle 0(t)|V^\alpha|0(t)\rangle$  with  $V^\alpha$  being time-independent, we can separate out the global phase from  $|0(t)\rangle$ ,

$$|0(t)\rangle = e^{i\theta(t)}|\tilde{0}(t)\rangle, \quad \theta(t)|_{V(t)=0} = -tE_0(\{\mathbf{R}_A\}). \quad (45)$$

We then define

$$A(t) = \langle \tilde{0}(t) | V^\alpha | \tilde{0}(t) \rangle, \quad (46)$$

which can be expanded as

$$A(t) = A^{(0)}(t) + A^{(1)}(t) + A^{(2)}(t) + \dots, \quad (47)$$

$$A^{(0)}(t) = \langle 0 | V^\alpha | 0 \rangle, \quad (48)$$

$$A^{(1)}(t) = \sum_k e^{-i\omega_k t} \sum_\beta A^\beta(\omega_k) \epsilon_\beta(\omega_k), \quad (49)$$

$$A^{(2)}(t) = \sum_{kl} e^{-i(\omega_k + \omega_l)t} \sum_{\beta\gamma} A^{\beta\gamma}(\omega_k, \omega_l) \epsilon_\beta(\omega_k) \epsilon_\gamma(\omega_l). \quad (50)$$

To derive the linear  $[A^\beta(\omega_k)]$  and quadratic  $[A^{\beta\gamma}(\omega_k, \omega_l)]$  response functions in the framework of TDDFT, we parameterize the phase-separated state  $|\tilde{0}(t)\rangle$  as

$$|\tilde{0}(t)\rangle = e^{-\kappa(t)} |0\rangle, \quad \kappa(t) = -\kappa^\dagger(t), \quad (51)$$

where  $\kappa(t)$  can be expanded as

$$\kappa(t) = \kappa^{(1)}(t) + \kappa^{(2)}(t) + \dots, \quad \kappa^{(0)}(t) = 0 \quad (52)$$

in accordance with Eq. (47). To determine  $\kappa(t)$ , we invoke Ehrenfest's theorem<sup>21</sup>

$$\langle 0 | [\hat{q}, e^{\kappa(t)} (H_{\text{KS}}(t) + V(t) - i \frac{\partial}{\partial t}) e^{-\kappa(t)} ] | 0 \rangle = 0, \quad (53)$$

where  $H_{\text{KS}}(t)$  is the KS operator and  $\hat{q}$  is an arbitrary operator in the operator basis used to expand  $O_I^\dagger$ , taken here to be  $a_p^\dagger a_q$ . Both Eq. (46) in conjunction with Eq. (51) and Eq. (53) possess operators of the form  $e^{\kappa(t)} O e^{-\kappa(t)}$ , which can be expanded as

$$e^{\kappa(t)} O e^{-\kappa(t)} = O + [\kappa(t), O] + \frac{1}{2} [\kappa(t), [\kappa(t), O]] + \dots. \quad (54)$$

It is interesting to note that, if only the first-order term of  $\kappa(t)$  is retained, applying the expansion (54) to Eq. (53) will yield the EOM (27), which is equivalent to the standard TDDFT (12). Likewise, repeating the same to Eq. (46) will recover the commutator type of metrics (29) and (31), thereby explaining the underlying reasoning for EOM to take such metrics. However,  $\kappa^{(2)}(t)$  also contributes to the *ee* fo-NACMEs, which is missed by the linear-response EOM (27). The contribution of  $\kappa^{(2)}(t)$  is to be determined by the quadratic response equation

$$(\mathbf{E} - \omega_{JI}\mathbf{S})\mathbf{t}_{IJ} = \mathbf{V}_{IJ}, \quad \mathbf{t}_{IJ} = \begin{pmatrix} \mathbf{X}_{IJ} \\ \mathbf{Y}_{IJ} \end{pmatrix}, \quad (55)$$

with  $\mathbf{V}_{IJ}$  defined by equation (32) of Ref. 14. The EOM *ee* fo-NACMEs (43) should hence be extended accordingly to

$$\langle I|\partial_\xi|J\rangle = \sum_{pq} \tilde{\gamma}_{pq}^{IJ} \langle \psi_p|\partial_\xi|\psi_q\rangle + \omega_{JI}^{-1} \mathbf{t}_I^\dagger (\partial_\xi \mathbf{E}) \mathbf{t}_J, \quad (56)$$

$$\tilde{\gamma}_{pq}^{IJ} = \tilde{\gamma}_{pq}^{IJ} + (\mathbf{X}_{IJ})_{pq} \delta_{pi} \delta_{qa} - (\mathbf{Y}_{IJ})_{qp} \delta_{qi} \delta_{pa}. \quad (57)$$

It turns out that the last, quadratic-response term does improve the accuracy of the *ee* fo-NACMEs but often introduces numerical instability and even divergence,<sup>14,16,17</sup> which arises whenever three TDDFT excitation energies  $\omega_I, \omega_J, \omega_K$  satisfy the three-state resonance condition  $\omega_I - \omega_J = \omega_K$ , thereby rendering the left-hand side of Eq. (55) singular. It has therefore been recommended<sup>14</sup> that the original EOM expression (43) for the *ee* fo-NACMEs should be used instead. Still, however, such TDPT-based formulation puts NAC-TDDFT on a firm basis, at least conceptually. Note in passing that this type of divergence is not limited to adiabatic TDDFT but is present in all approximate theories.<sup>22</sup>

### 3 Proper implementation

Having discussed the essentials of NAC-TDDFT, we comment briefly on the actual implementation. The major issue here is how to handle the implicit dependence of the MOs on the nuclear coordinates imposed by the Brillouin and orthonormality conditions

$$F_{ia} = 0; \quad S_{pq} = \delta_{pq}. \quad (58)$$

To transform the nuclear derivatives of the MOs into a tractable form, we first note that the fo-NACMEs can be interpreted as the nuclear derivatives of some function. For example, Eqs. (42) and (43) are, respectively, the total derivatives of

$$g_{0I}(\{\mathbf{R}_A\}, \mathbf{C}(\{\mathbf{R}_A\})) = \sum_{ia} (\mathbf{X}_I - \mathbf{Y}_I)_{ia} \langle \psi_i(\{\mathbf{R}_A\}_0) | \psi_a(\{\mathbf{R}_A\}) \rangle, \quad (59)$$

and

$$g_{IJ}(\{\mathbf{R}_A\}, \mathbf{C}(\{\mathbf{R}_A\})) = \sum_{pq} \tilde{\gamma}_{pq}^{IJ} \langle \psi_p(\{\mathbf{R}_A\}_0) | \psi_q(\{\mathbf{R}_A\}) \rangle + \omega_{JI}^{-1} \mathbf{t}_I^\dagger \mathbf{E}(\{\mathbf{R}_A\}) \mathbf{t}_J, \quad (60)$$

with respect to  $\{\mathbf{R}_A\}$  at the expansion point  $\{\mathbf{R}_A\}_0$ . That is, only the ket of  $\langle \psi_p | \psi_q \rangle$  is to be differentiated. The next step is to introduce a suitable Lagrangian incorporating explicitly the constraints (58)

$$\begin{aligned} L[\{\mathbf{R}_A\}, \mathbf{C}(\{\mathbf{R}_A\}), \mathbf{Z}, \mathbf{W}] &= g(\{\mathbf{R}_A\}, \mathbf{C}(\{\mathbf{R}_A\})) + \sum_{ia} Z_{ia} F_{ia}(\mathbf{C}(\{\mathbf{R}_A\})) \\ &\quad - \sum_{pq} W_{pq} (S_{pq}(\mathbf{C}(\{\mathbf{R}_A\})) - \delta_{pq}), \end{aligned} \quad (61)$$

so as to eliminate the need to differentiate the MO coefficients  $\mathbf{C}(\{\mathbf{R}_A\})$  with respect to  $\{\mathbf{R}_A\}$ . This is achieved by requiring the Lagrangian to be stationary with respect to  $\mathbf{C}(\{\mathbf{R}_A\})$ ,  $\mathbf{Z}$ , and  $\mathbf{W}$  (but not with respect to  $\mathbf{C}(\{\mathbf{R}_A\}_0)$ !), such that  $\mathbf{C}(\{\mathbf{R}_A\})$  can be treated as an independent, unconstrained variational parameter rather than a parameter

that depends on  $\{\mathbf{R}_A\}$ . Consequently, the fo-NACMEs take simply the following form

$$g^\xi = \frac{dL}{d\xi} = \frac{\partial L}{\partial \xi} = \frac{\partial g}{\partial \xi} + \sum_{ia} Z_{ia} \frac{\partial F_{ia}}{\partial \xi} - \sum_{pq} W_{pq} \frac{\partial S_{pq}}{\partial \xi}, \quad (62)$$

where the first equality arises because the last two terms of Eq. (61) are zero when the stationary conditions with respect to  $\mathbf{Z}$  and  $\mathbf{W}$  are fulfilled, whereas the second equality is due to that the dependence of  $L$  on  $\{\mathbf{R}_A\}$  is completely explicit (for a detailed discussion of the Lagrangian technique, see Appendix B of Ref. 23).

The Lagrange multipliers  $\mathbf{Z}$  and  $\mathbf{W}$  are determined by the stationary condition of  $L$  with respect to  $\mathbf{C}(\{\mathbf{R}_A\})$  (see equations (74)-(80) in Ref. 14). In particular, the Z-vector equation

$$(\mathbf{A} + \mathbf{B})\mathbf{Z} = \mathbf{X}_I - \mathbf{Y}_I \quad (63)$$

for the TDDFT *ge* fo-NACMEs can be solved directly

$$\mathbf{Z} = (\mathbf{A} + \mathbf{B})^{-1}(\mathbf{X}_I - \mathbf{Y}_I) = \omega_I^{-1}(\mathbf{X}_I + \mathbf{Y}_I). \quad (64)$$

Ironically, the TDA version of Eq. (63)

$$(\mathbf{A} + \mathbf{B})\mathbf{Z} = \mathbf{X}_I \quad (65)$$

has to be solved explicitly. As a result, the TDA *ge* fo-NACMEs are more expensive to compute than those of full TDDFT. Actually, the computational cost of the TDDFT *ge* fo-NACMEs is very similar to that of the DFT gradients (which also do not involve solving a Z-vector equation due to their variational nature), with only one additional complication: the integrals  $\langle \mu | \partial_\xi | \nu \rangle$  in  $\langle \psi_p | \partial_\xi | \psi_q \rangle$  must be evaluated in a way that ensures translational invariance.<sup>24</sup>

At this point, it deserves to be mentioned that, in the CBS limit, the derivatives  $\frac{\partial F_{ia}}{\partial \xi}$  in

Eq. (62) reduce to  $\langle \psi_i | V_{\text{ne}}^\xi | \psi_a \rangle$ , while all other terms therein vanish, thereby reproducing the Hellmann-Feynman-like expression (11). In view of Eq. (17), the  $V_{\text{ne}}$  contribution to  $\frac{\partial E_{ia}}{\partial \xi}$  reads

$$\frac{\partial}{\partial \xi} \langle \psi_i | V_{\text{ne}} | \psi_a \rangle = \sum_{\mu\nu} C_{\mu i} \frac{\partial}{\partial \xi} \langle \mu | V_{\text{ne}} | \nu \rangle C_{\nu a}. \quad (66)$$

Since the basis set representation of  $V_{\text{ne}}$  is much easier than that of  $V_{\text{ne}}^\xi$ , it is clear that Eq. (62) converges much faster than Eq. (11). In particular, no special basis functions<sup>3</sup> are needed, which is a point that should have been expected from the very beginning, for the fo-NACMEs are valence properties anyway.

Finally, the computational cost of the *ee* fo-NACMEs is very similar to that of the TDDFT gradients,<sup>23,25,26</sup> as already noticed before.<sup>14</sup> There is a simple reason for this: the second term of Eq. (60) resembles closely the TDDFT excitation energy  $\omega_I = \mathbf{t}_I^\dagger \mathbf{E}(\{\mathbf{R}_A\}) \mathbf{t}_I$ , such that the TDDFT *ee* fo-NACMEs can readily be implemented in a code that already supports TDDFT gradients.

## 4 Illustration

Azulene is known as a textbook example of anti-Kasha fluorescence. That is, the  $S_2 \rightarrow S_1$  internal conversion (IC) therein is not fast enough to quench completely the  $S_2 \rightarrow S_0$  fluorescence, while the  $S_1 \rightarrow S_0$  IC is sufficiently fast to make the  $S_1$  state nearly non-fluorescent, thereby leading to a fluorescence dominated by  $S_2$  instead of  $S_1$ .<sup>27-31</sup> As such, azulene is an ideal model for the study of IC phenomena. For this reason, it is taken here as a showcase to reveal the performance of NAC-TDDFT in different flavors. Since the AWF-based NAC-TDDFT is not at our disposal, we only report results by using the Hellmann-Feynman-like formula (11),<sup>2</sup> the EOM expressions (42) and (43),<sup>13,14</sup> as well as the TDPT ones (42) and (56).<sup>13,14</sup> For the *ee* fo-NACMEs described by Eq. (11), both the EOM rTDM  $\tilde{\gamma}^{IJ}$  in Eq. (38) and the TDPT rTDM  $\tilde{\gamma}^{IJ}$  in Eq. (57) were tested, with the corresponding results denoted as  $g^{\xi, \text{CBS(EOM)}}$  and  $g^{\xi, \text{CBS(TDPT)}}$ , respectively. The  $S_0$ - $S_1$ ,  $S_1$ - $S_2$ , and  $T_1$ - $T_2$

fo-NACMEs of azulene were computed with the BDF program package,<sup>32–36</sup> at the  $S_1$ ,  $S_2$  and  $T_2$  equilibrium geometries (optimized with B3LYP<sup>37,38</sup>/def2-SVP<sup>39</sup>), respectively. The response calculations employed the B3LYP collinear spin-flip exchange-correlation kernel, for the noncollinear kernel<sup>40–42</sup> has not yet been interfaced with the NAC-TDDFT module in BDF.

The first thing to note is the basis set convergence rates of the three methods. To this end, the def2-SV(P), def2-SVP, def2-TZVP, and def2-TZVPP basis sets<sup>39</sup> were used, with the results documented in Table 1. As can be seen, the root-mean-square (RMS) deviations of the EOM and TDPT fo-NACMEs from the near CBS results are smaller by 2 to 3 orders of magnitude than those by Eq. (11). Notably, while  $g^{\xi, \text{CBS}(\text{TDPT})}$  approaches slowly  $g^{\xi, \text{TDPT}}(\text{def2-TZVPP})$  as the basis set is enlarged,  $g^{\xi, \text{CBS}(\text{EOM})}$  does not approach  $g^{\xi, \text{EOM}}(\text{def2-TZVPP})$  and grossly overestimates the fo-NACMEs compared with both  $g^{\xi, \text{EOM}}$  and  $g^{\xi, \text{TDPT}}$  (cf. Fig. 1). In fact, it can be proven<sup>13</sup> that  $g^{\xi, \text{CBS}(\text{TDPT})}$  (for *ee* fo-NACMEs) coincides with  $g^{\xi, \text{TDPT}}$ , but  $g^{\xi, \text{CBS}(\text{EOM})}$  in general does not agree with  $g^{\xi, \text{EOM}}$  in the CBS limit. Therefore, from both numerical and theoretical points of view,  $g^{\xi, \text{CBS}(\text{EOM})}$  should not be recommended as a useful approach.

The overall accuracy of the calculated fo-NACME can be assessed by their use in computing the IC rate constants (at  $T = 300$  K) of  $S_1 \rightarrow S_0$ ,  $S_2 \rightarrow S_1$ , and  $T_2 \rightarrow T_1$ . The MOMAP software package<sup>43–45</sup> was used here, with Duschinsky rotation effects accounted for. The harmonic vibrational frequencies were derived from the numerical Hessian yet based on analytically evaluated TDDFT/B3LYP/def2-SVP gradients<sup>23</sup> available in BDF. The results are collected in Table 2, to be compared with the experimental values ( $5.3 \times 10^{11} \text{ s}^{-1}$  for  $S_1 \rightarrow S_0$ <sup>27</sup> and  $3.5 \times 10^8 \text{ s}^{-1}$  for  $S_2 \rightarrow S_1$ <sup>28,29</sup>). It appears that all methods tend to underestimate the IC rate constant of  $S_1 \rightarrow S_0$ , which undergoes mainly through a conical intersection.<sup>30</sup> However, this cannot be fully ascribed to the quality of the calculated fo-NACMEs, since the harmonic approximation for the vibrations also tends to underestimate the rate constant of processes through conical intersections (CX). Such argument is



supported by the fact that the rate constant of the non-CX  $S_2 \rightarrow S_1$  is well reproduced by both the EOM and TDPT based approaches. In contrast, both  $k_{S_2 \rightarrow S_1}^{\text{CBS(TDPT)}}$  and especially  $k_{S_2 \rightarrow S_1}^{\text{CBS(EOM)}}$  are in large errors, showing again that the Hellmann-Feynman-like expression (11) is unreliable. The  $T_2 \rightarrow T_1$  IC turns out to be orders of magnitude faster than both  $S_2 \rightarrow S_1$  and  $S_1 \rightarrow S_0$ , due to a much smaller energy gap (0.29, 1.34, and 1.59 eV for  $T_2$ - $T_1$ ,  $S_2$ - $S_1$ , and  $S_1$ - $S_0$ , respectively). Because of this, the  $T_2 \rightarrow T_1$  IC cannot readily be detected experimentally.

## 5 Conclusions and outlook

Different formulations of NAC-TDDFT for the fo-NACMEs between the ground and excited states and between two excited states have been analyzed critically and demonstrated numerically. The take-home messages include (1) the Hellmann-Feynman type of formulation is hardly useful due to huge demands on basis sets; (2) the AWF-based formulation is not theoretically founded and may give incorrect expressions; (3) the TDPT-based formulation is most rigorous but the quadratic responses therein may be problematic, not because of the formulation itself but due to the approximate nature of the exchange-correlation kernel; (4) the EOM-based formulation is not only elegant but is also free of numerical instabilities, and is therefore the recommended choice. Further extensions of the EOM variant of NAC-TDDFT include (a) use of fragment localized molecular orbitals<sup>46-49</sup> for efficient calculations of large systems; (b) combination with spin adaptation<sup>23,50-52</sup> for proper treatment of open-shell systems; (c) combination with perturbative treatment of SOC,<sup>53-55</sup> which is another source for nonadiabatic couplings; and (d) combination with variational treatment of SOC<sup>7,41,42,56-60</sup> for systems containing very heavy elements. Progresses along these directions are being made at our laboratory.

## ACKNOWLEDGMENTS

This work was supported by the National Key R&D Program of China (Grant No. 2017YFB0203402), National Natural Science Foundation of China (Grant Nos. 21833001 and 21973054), Mountain Tai Climb Program of Shandong Province, and Key-Area Research and Development Program of Guangdong Province (Grant No. 2020B0101350001).

## BIOGRAPHICAL INFORMATION

**Z. Wang** was born in 1995 and obtained his Ph. D. in Chemistry from Peking University (2018). His research interests include spin-adapted open-shell time-dependent density functional theory, fragmentation and semiempirical methods.

**C. Wu** was born in 1994 and obtained his Ph. D. in Chemistry from University of New South Wales (2020). His research focuses on computer-aided rational design of organic dyes and photocatalysts for polymerization.

**W. Liu** is Chair Professor at Shandong University, member of International Academy of Quantum Molecular Science, fellow of Royal Society of Chemistry and Asia-Pacific Association of Theoretical and Computational Chemists, recipient of Bessel Award of Humboldt Foundation, Annual Medal of International Academy of Quantum Molecular Science, Pople and Fukui Medals of Asia-Pacific Association of Theoretical and Computational Chemists. His research interests include quantum electrodynamics, relativistic electronic structure theory, many-body theory of strong correlation, time-dependent density functional theory, etc.

## References

- 1 Cotton, S. J.; Liang, R.; Miller, W. H. On the adiabatic representation of Meyer-Miller electronic-nuclear dynamics. *J. Chem. Phys.* **2017**, *147*, 064112.
- 2 Chernyak, V.; Mukamel, S. Density-matrix representation of nonadiabatic couplings in

- time-dependent density functional (TDDFT) theories. *J. Chem. Phys.* **2000**, *112*, 3572–3579.
- 3 Send, R.; Furche, F. First-order nonadiabatic couplings from time-dependent hybrid density functional response theory: Consistent formalism, implementation, and performance. *J. Chem. Phys.* **2010**, *132*, 044107.
  - 4 Lee, S.; Kim, E.; Lee, S.; Choi, C. H. Fast overlap evaluations for nonadiabatic molecular dynamics simulations: Applications to SF-TDDFT and TDDFT. *J. Chem. Theory Comput.* **2019**, *15*, 882–891.
  - 5 Lee, S.; Horbatenko, Y.; Filatov, M.; Choi, C. H. Fast and Accurate Computation of Nonadiabatic Coupling Matrix Elements Using the Truncated Leibniz Formula and Mixed-Reference Spin-Flip Time-Dependent Density Functional Theory. *J. Phys. Chem. Lett.* **2021**, *12*, 4722–4728.
  - 6 Casida, M. E. In *Recent Advances In Density Functional Methods: (Part I)*; Chang, D. P., Ed.; World Scientific: Singapore, 1995; pp 155–192.
  - 7 Liu, W.; Xiao, Y. Relativistic time-dependent density functional theories. *Chem. Soc. Rev.* **2018**, *47*, 4481–4509.
  - 8 Tapavicza, E.; Tavernelli, I.; Rothlisberger, U. Trajectory Surface Hopping within Linear Response Time-Dependent Density-Functional Theory. *Phys. Rev. Lett.* **2007**, *98*, 023001.
  - 9 Hu, C.; Hirai, H.; Sugino, O. Nonadiabatic couplings from time-dependent density functional theory: Formulation in the Casida formalism and practical scheme within modified linear response. *J. Chem. Phys.* **2007**, *127*, 064103.
  - 10 Hu, C.; Sugino, O.; Hirai, H.; Tateyama, Y. Nonadiabatic couplings from the Kohn-

- Sham derivative matrix: Formulation by time-dependent density-functional theory and evaluation in the pseudopotential framework. *Phys. Rev. A* **2010**, *82*, 062508.
- 11 Tavernelli, I.; Curchod, B. F. E.; Laktionov, A.; Rothlisberger, U. Nonadiabatic coupling vectors for excited states within time-dependent density functional theory in the Tamm–Dancoff approximation and beyond. *J. Chem. Phys.* **2010**, *133*, 194104.
  - 12 Alguire, E. C.; Ou, Q.; Subotnik, J. E. Calculating Derivative Couplings between Time-Dependent Hartree–Fock Excited States with Pseudo-Wavefunctions. *J. Phys. Chem. B* **2015**, *119*, 7140–7149.
  - 13 Li, Z.; Liu, W. First-order nonadiabatic coupling matrix elements between excited states: A Lagrangian formulation at the CIS, RPA, TD-HF, and TD-DFT levels. *J. Chem. Phys.* **2014**, *141*, 014110.
  - 14 Li, Z.; Suo, B.; Liu, W. First order nonadiabatic coupling matrix elements between excited states: Implementation and application at the TD-DFT and pp-TDA levels. *J. Chem. Phys.* **2014**, *141*, 244105.
  - 15 Zhang, X.; Lu, G. First-order nonadiabatic couplings in extended systems by time-dependent density functional theory. *J. Chem. Phys.* **2018**, *149*, 244103.
  - 16 Ou, Q.; Bellchambers, G. D.; Furche, F.; Subotnik, J. E. First-order derivative couplings between excited states from adiabatic TDDFT response theory. *J. Chem. Phys.* **2015**, *142*, 064114.
  - 17 Zhang, X.; Herbert, J. M. Analytic derivative couplings in time-dependent density functional theory: Quadratic response theory versus pseudo-wavefunction approach. *J. Chem. Phys.* **2015**, *142*, 064109.
  - 18 Rowe, D. J. Equations-of-Motion Method and the Extended Shell Model. *Rev. Mod. Phys.* **1968**, *40*, 153–166.

- 19 Etienne, T. Auxiliary many-body wavefunctions for TDDFRT electronic excited states: Consequences for the representation of molecular electronic transitions. *arXiv preprint arXiv:2104.13616* **2021**,
- 20 Luzanov, A. V.; Zhikol, O. A. Electron invariants and excited state structural analysis for electronic transitions within CIS, RPA, and TDDFT models. *Int. J. Quantum Chem.* **2010**, *110*, 902–924.
- 21 Olsen, J.; Jørgensen, P. Linear and nonlinear response functions for an exact state and for an MCSCF state. *J. Chem. Phys.* **1985**, *82*, 3235–3264.
- 22 Parker, S. M.; Roy, S.; Furche, F. Unphysical divergences in response theory. *J. Chem. Phys.* **2016**, *145*, 134105.
- 23 Wang, Z.; Li, Z.; Zhang, Y.; Liu, W. Analytic energy gradients of spin-adapted open-shell time-dependent density functional theory. *J. Chem. Phys.* **2020**, *153*, 164109.
- 24 Fatehi, S.; Alguire, E.; Shao, Y.; Subotnik, J. E. Analytic derivative couplings between configuration-interaction-singles states with built-in electron-translation factors for translational invariance. *J. Chem. Phys.* **2011**, *135*, 234105.
- 25 Furche, F.; Ahlrichs, R. Adiabatic time-dependent density functional methods for excited state properties. *J. Chem. Phys.* **2002**, *117*, 7433–7447.
- 26 Furche, F.; Ahlrichs, R. Erratum: “Time-dependent density functional methods for excited state properties” [*J. Chem. Phys.* 117, 7433 (2002)]. *J. Chem. Phys.* **2004**, *121*, 12772–12773.
- 27 Ippen, E. P.; Shank, C. V.; Woerner, R. L. Picosecond dynamics of azulene. *Chem. Phys. Lett.* **1977**, *46*, 20–23.
- 28 Hirata, Y.; Lim, E. C. Radiationless transitions in azulene: Evidence for the ultrafast S<sub>2</sub>→S<sub>0</sub> internal conversion. *J. Chem. Phys.* **1978**, *69*, 3292–3296.

- 29 Wagner, B. D.; Tittelbach-Helmrich, D.; Steer, R. P. Radiationless decay of the S2 states of azulene and related compounds: solvent dependence and the energy gap law. *J. Phys. Chem.* **1992**, *96*, 7904–7908.
- 30 Amatatsu, Y.; Komura, Y. Reaction coordinate analysis of the S1-S0 internal conversion of azulene. *J. Chem. Phys.* **2006**, *125*, 174311.
- 31 Beer, M.; Longuet-Higgins, H. C. Anomalous Light Emission of Azulene. *J. Chem. Phys.* **1955**, *23*, 1390–1391.
- 32 Liu, W.; Hong, G.; Dai, D.; Li, L.; Dolg, M. The Beijing 4-component density functional theory program package (BDF) and its application to EuO, EuS, YbO and YbS. *Theor. Chem. Acc.* **1997**, *96*, 75–83.
- 33 Liu, W.; Wang, F.; Li, L. The Beijing Density Functional (BDF) program package: Methodologies and applications. *J. Theor. Comput. Chem.* **2003**, *2*, 257–272.
- 34 Liu, W.; Wang, F.; Li, L. In *Recent Advances in Relativistic Molecular Theory*; Hirao, K., Ishikawa, Y., Eds.; World Scientific: Singapore, 2004; pp 257–282.
- 35 Liu, W.; Wang, F.; Li, L. In *Encyclopedia of Computational Chemistry*; von Ragué Schleyer, P., Allinger, N. L., Clark, T., Gasteiger, J., Kollman, P. A., Schaefer III, H. F., Eds.; Wiley: Chichester, UK, 2004.
- 36 Zhang, Y. et al. BDF: A relativistic electronic structure program package. *J. Chem. Phys.* **2020**, *152*, 064113.
- 37 Becke, A. D. Density-functional thermochemistry. III. The role of exact exchange. *J. Chem. Phys.* **1993**, *98*, 5648.
- 38 Stephens, P. J.; Devlin, F. J.; Chabalowski, C. F.; Frisch, M. J. AB-INITIO CALCULATION OF VIBRATIONAL ABSORPTION AND CIRCULAR-DICHROISM SPECTRA USING DENSITY-FUNCTIONAL FORCE-FIELDS. *J. Phys. Chem.* **1994**, *98*, 11623.

- 39 Weigend, F.; Ahlrichs, R. Balanced basis sets of split valence, triple zeta valence and quadruple zeta valence quality for H to Rn: Design and assessment of accuracy. *Phys. Chem. Chem. Phys.* **2005**, *7*, 3297–3305.
- 40 Wang, F.; Liu, W. Comparison of Different Polarization Schemes in Open-shell Relativistic Density Functional Calculations. *J. Chin. Chem. Soc. (Taipei)* **2003**, *50*, 597–606.
- 41 Gao, J.; Liu, W.; Song, B.; Liu, C. Time-dependent four-component relativistic density functional theory for excitation energies. *J. Chem. Phys.* **2004**, *121*, 6658–6666.
- 42 Gao, J.; Zou, W.; Liu, W.; Xiao, Y.; Peng, D.; Song, B.; Liu, C. Time-dependent four-component relativistic density-functional theory for excitation energies. II. The exchange-correlation kernel. *J. Chem. Phys.* **2005**, *123*, 054102.
- 43 Niu, Y.; Li, W.; Peng, Q.; Geng, H.; Yi, Y.; Wang, L.; Nan, G.; Wang, D.; Shuai, Z. MOlecular MAterials Property Prediction Package (MOMAP) 1.0: a software package for predicting the luminescent properties and mobility of organic functional materials. *Mol. Phys.* **2018**, *116*, 1078–1090.
- 44 Peng, Q.; Yi, Y.; Shuai, Z.; Shao, J. Excited state radiationless decay process with Duschinsky rotation effect: Formalism and implementation. *J. Chem. Phys.* **2007**, *126*, 114302.
- 45 Niu, Y.; Peng, Q.; Shuai, Z. Promoting-mode free formalism for excited state radiationless decay process with Duschinsky rotation effect. *Sci. China Ser. B: Chem.* **2008**, *51*, 1153–1158.
- 46 Wu, F.; Liu, W.; Zhang, Y.; Li, Z. Linear-Scaling Time-Dependent Density Functional Theory Based on the Idea of “From Fragments to Molecule”. *J. Chem. Theory Comput.* **2011**, *7*, 3643–3660.

- 47 Liu, J.; Zhang, Y.; Liu, W. Photoexcitation of Light-Harvesting C–P–C60 Triads: A FLMO-TD-DFT Study. *J. Chem. Theory Comput.* **2014**, *10*, 2436–2448.
- 48 Li, Z.; Li, H.; Suo, B.; Liu, W. Localization of Molecular Orbitals: From Fragments to Molecule. *Acc. Chem. Res.* **2014**, *47*, 2758–2767.
- 49 Li, H.; Liu, W.; Suo, B. Localization of open-shell molecular orbitals via least change from fragments to molecule. *J. Chem. Phys.* **2017**, *146*, 104104.
- 50 Li, Z.; Liu, W. Spin-adapted open-shell random phase approximation and time-dependent density functional theory. I. Theory. *J. Chem. Phys.* **2010**, *133*, 064106.
- 51 Li, Z.; Liu, W.; Zhang, Y.; Suo, B. Spin-adapted open-shell time-dependent density functional theory. II. Theory and pilot application. *J. Chem. Phys.* **2011**, *134*, 134101.
- 52 Li, Z.; Liu, W. Spin-adapted open-shell time-dependent density functional theory. III. An even better and simpler formulation. *J. Chem. Phys.* **2011**, *135*, 194106, (E)**138**, 029904 (2013).
- 53 Li, Z.; Xiao, Y.; Liu, W. On the spin separation of algebraic two-component relativistic Hamiltonians. *J. Chem. Phys.* **2012**, *137*, 154114.
- 54 Li, Z.; Xiao, Y.; Liu, W. On the spin separation of algebraic two-component relativistic Hamiltonians: Molecular properties. *J. Chem. Phys.* **2014**, *141*, 054111.
- 55 Li, Z.; Suo, B.; Zhang, Y.; Xiao, Y.; Liu, W. Combining spin-adapted open-shell TD-DFT with spin-orbit coupling. *Mol. Phys.* **2013**, *111*, 3741–3755.
- 56 Peng, D.; Zou, W.; Liu, W. Time-dependent quasirelativistic density-functional theory based on the zeroth-order regular approximation. *J. Chem. Phys.* **2005**, *123*, 144101.
- 57 Xu, W.; Zhang, Y.; Liu, W. Time-dependent relativistic density functional study of Yb and YbO. *Sci. China Ser. B: Chem.* **2009**, *52*, 1945–1953.



- 58 Xu, W.; Ma, J.; Peng, D.; Zou, W.; Liu, W.; Staemmler, V. Excited states of ReO<sub>4</sub><sup>-</sup>: A comprehensive time-dependent relativistic density functional theory study. *Chem. Phys.* **2009**, *356*, 219–228.
- 59 Zhang, Y.; Xu, W.; Sun, Q.; Zou, W.; Liu, W. Excited states of OsO<sub>4</sub>: A comprehensive time-dependent relativistic density functional theory study. *J. Comput. Chem.* **2010**, *31*, 532–551.
- 60 Liu, W. Essentials of relativistic quantum chemistry. *J. Chem. Phys.* **2020**, *152*, 180901.

Table 1: Root-mean-square deviations of TDDFT/B3LYP fo-NACMEs (in Bohr<sup>-1</sup>) between different states of azulene from the reference data:  $g^{\xi,\text{EOM}}(\text{def2-TZVPP})$  for  $g^{\xi,\text{EOM}}$  and  $g^{\xi,\text{CBS(EOM)}}$ , and  $g^{\xi,\text{TDPT}}(\text{def2-TZVPP})$  for  $g^{\xi,\text{TDPT}}$  and  $g^{\xi,\text{CBS(TDPT)}}$ .  $g^{\xi,\text{EOM}}$  by Eq. (42)/(43);  $g^{\xi,\text{TDPT}}$  by Eq. (42)/(56);  $g^{\xi,\text{CBS(EOM)}}$  by Eq. (11) with  $\tilde{\gamma}^{IJ}$  (38);  $g^{\xi,\text{CBS(TDPT)}}$  by Eq. (11) with  $\tilde{\gamma}^{IJ}$  (57).

	def2-SV(P)	def2-SVP	def2-TZVP	def2-TZVPP
$g_{S_0S_1}^{\xi,\text{EOM}}$	0.0037	0.0006	0.0002	0.0000
$g_{S_0S_1}^{\xi,\text{CBS(EOM)}}$	0.1077	0.1072	0.0601	0.0585
$g_{S_1S_2}^{\xi,\text{EOM}}$	0.0028	0.0031	0.0003	0.0000
$g_{S_1S_2}^{\xi,\text{TDPT}}$	0.0037	0.0042	0.0003	0.0000
$g_{S_1S_2}^{\xi,\text{CBS(EOM)}}$	0.4774	0.4746	0.4949	0.4941
$g_{S_1S_2}^{\xi,\text{CBS(TDPT)}}$	0.0865	0.0841	0.0523	0.0505
$g_{T_1T_2}^{\xi,\text{EOM}}$	0.0726	0.0775	0.0039	0.0000
$g_{T_1T_2}^{\xi,\text{TDPT}}$	0.0724	0.0774	0.0039	0.0000
$g_{T_1T_2}^{\xi,\text{CBS(EOM)}}$	1.5479	1.5688	1.4715	1.4685
$g_{T_1T_2}^{\xi,\text{CBS(TDPT)}}$	0.4406	0.4356	0.2514	0.2419

Table 2: TDDFT/B3LYP internal conversion rate constants ( $k$  in  $\text{s}^{-1}$ ) between different states of azulene. The experimental values are  $5.3 \times 10^{11} \text{ s}^{-1}$  for  $k_{S_1 \rightarrow S_0}$ <sup>27</sup> and  $3.5 \times 10^8 \text{ s}^{-1}$  for  $k_{S_2 \rightarrow S_1}$ .<sup>28,29</sup> For additional explanations, see Table 1.

	def2-SV(P)	def2-SVP	def2-TZVP	def2-TZVPP
$k_{S_1 \rightarrow S_0}^{\text{EOM}}$	7.96E+08	8.00E+08	7.67E+08	7.68E+08
$k_{S_1 \rightarrow S_0}^{\text{CBS(EOM)}}$	1.27E+09	1.32E+09	1.05E+09	1.04E+09
$k_{S_2 \rightarrow S_1}^{\text{EOM}}$	1.29E+09	1.27E+09	1.25E+09	1.25E+09
$k_{S_2 \rightarrow S_1}^{\text{TDPT}}$	1.38E+09	1.36E+09	1.35E+09	1.34E+09
$k_{S_2 \rightarrow S_1}^{\text{CBS(EOM)}}$	1.25E+10	1.26E+10	1.31E+10	1.31E+10
$k_{S_2 \rightarrow S_1}^{\text{CBS(TDPT)}}$	2.25E+09	2.44E+09	1.96E+09	1.94E+09
$k_{T_2 \rightarrow T_1}^{\text{EOM}}$	1.40E+13	1.42E+13	1.23E+13	1.22E+13
$k_{T_2 \rightarrow T_1}^{\text{TDPT}}$	1.39E+13	1.41E+13	1.22E+13	1.21E+13
$k_{T_2 \rightarrow T_1}^{\text{CBS(EOM)}}$	8.75E+13	8.92E+13	8.14E+13	8.11E+13
$k_{T_2 \rightarrow T_1}^{\text{CBS(TDPT)}}$	2.33E+13	2.33E+13	1.78E+13	1.74E+13

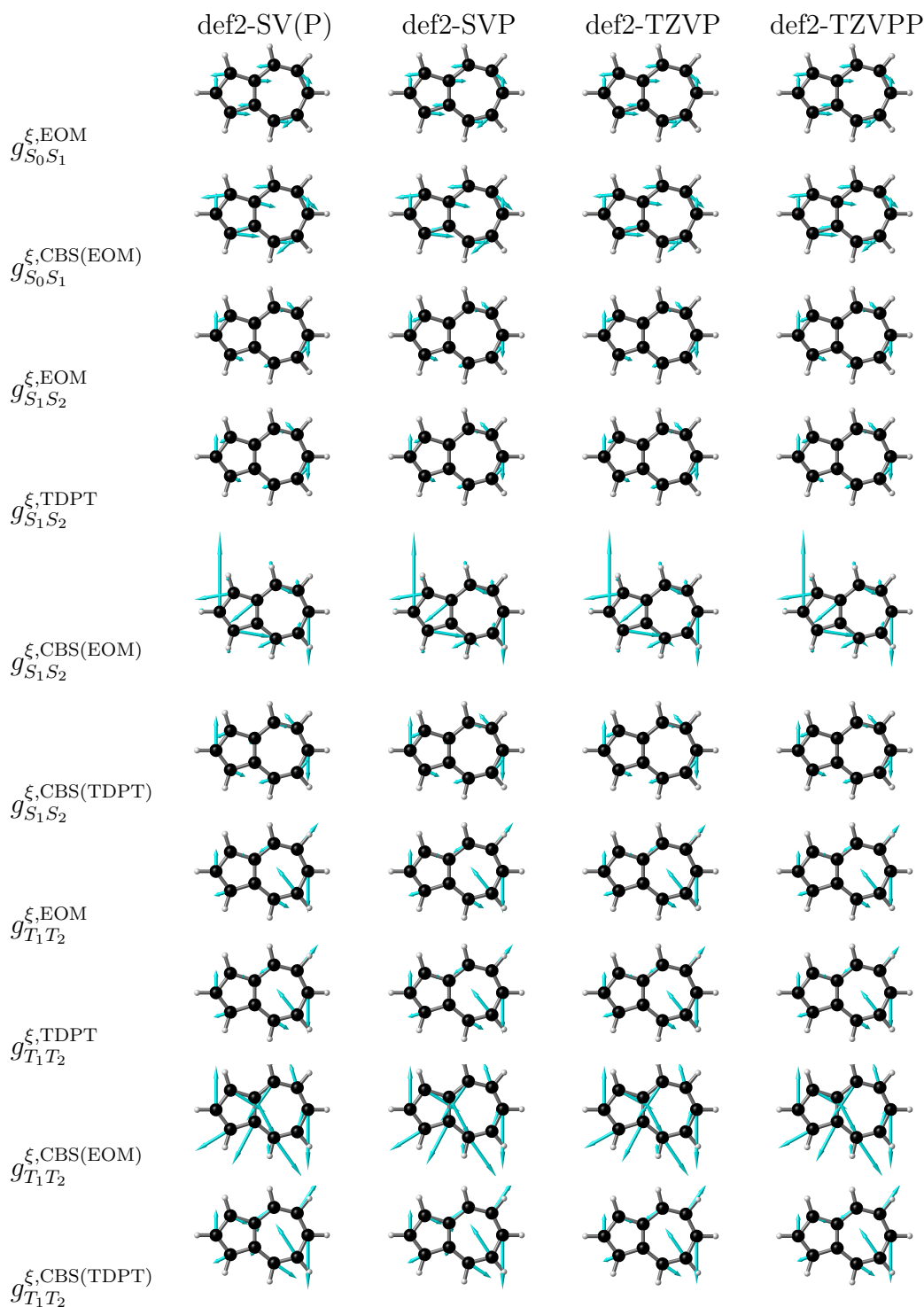


Figure 1: The  $S_0$ - $S_1$ ,  $S_1$ - $S_2$ , and  $T_1$ - $T_2$  fo-NACME vectors of azulene calculated by TDDFT/B3LYP with different basis sets (NB: the  $T_1$ - $T_2$  vectors are scaled by a factor of 1/3). For additional explanations, see Table 1.